View metadata, citation and similar papers at core.ac.uk

brought to you by CORE

provided by Okayama University Scientific Achievement Repository

Engineering

Electrical Engineering fields

Okayama University *Year* 1998

Rotor position estimation based on magnetic saliency of an IPM motor-realization of a wide-speed range from zero to the rated speed

Satoshi Ogasawara
Okayama University

Hirofumi Akagi
Okayama University

This paper is posted at eScholarship@OUDIR : Okayama University Digital Information Repository.

http://escholarship.lib.okayama-u.ac.jp/electrical_engineering/39

Rotor Position Estimation Based on Magnetic Saliency of an IPM Motor

— Realization of a Wide-Speed Range from Zero to the Rated Speed —

Satoshi Ogasawara, *Senior Member, IEEE*, and Hirofumi Akagi, *Fellow, IEEE*
Okayama University
3-1-1 Tsushima-Naka, Okayama, 700 JAPAN

Abstract— **This paper describes position estimation based on magnetic saliency of an interior permanent magnet synchronous motor (IPM motor) for the purpose of achieving a wide-speed range. The position estimation, which has been proposed by the authors, is characterized by the real-time algorithm estimating the rotor position at every PWM period. Selection of PWM patterns proposed in this paper expands the speed range capable of estimating the rotor position to a higher-speed range. The PWM patterns are switched over, depending on an amplitude and phase of the average output voltage vector. Experimental results obtained from an IPM motor drive system of 100 W demonstrate that the selection of the PWM patterns makes it possible to estimate the rotor position in a wide-speed range from zero to the rated speed.**

I. Introduction

In recent years, much attention has been paid to advanced sensorless drive systems that have the capability of controlling position, speed and/or torque of an ac motor from a standstill to a high-speed range without any shaft-mounted sensors. Some schemes based on high-frequency signal injection have been proposed to estimate rotor position or flux position of an ac motor [1]-[6].

The authors have proposed an approach to real-time position estimation based on magnetic saliency of an interior permanent magnet synchronous motor (IPM motor). The approach, without any special signal injection, is capable of calculating the inductance matrix including the information of the rotor position from current harmonics produced by switching operation of a PWM inverter driving the IPM motor. As a result, the rotor position can be estimated at every period of pulse-width-modulation [7].

Furthermore, an experimental position control system has been implemented and tested, introducing a novel PWM scheme using redundant voltage vectors to estimate the rotor position in a lower-speed range including standstill. Some experimental results have shown that the experimental system has the function of electrically locking the loaded motor shaft, and provides a position response as fast as about 20 rad/s [8]. However, in the case of using only a PWM pattern consisting of six non-zero voltage vectors, the maximum output voltage of the PWM inverter is restricted to half of the rated voltage.

This paper aims at expanding the speed range capable of estimating the rotor position to the higher-speed range, applying the approach to real-time position estimation based on magnetic saliency. When the amplitude of a voltage reference vector is larger than half of the rated voltage, the controller selects a suitable PWM pattern among six PWM patterns each of which contains four voltage vectors including a zero vector. As a result, the selection of the PWM pattern makes it possible to drive an IPM motor and to estimate the rotor position in a wide-speed range from zero to the rated speed. An experimental system consisting of a 100-W IPM motor and a voltage-source PWM inverter is constructed to confirm the effectiveness and versatility of the switchover of the PWM patterns. Experimental results show that excellent position-estimating characteristics are achieved over a wide speed range from zero to the rated speed (1500 rpm).

This paper also discusses accuracy of position estimation based on magnetic saliency. Analytical results show estimation errors that are originated from quantization error of an A/D converter, magnetic saliency ratio, and gain errors in a current sensor and an analog circuit.

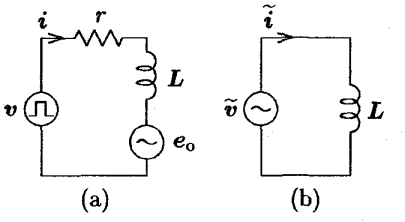

Fig. 1. Equivalent circuit of an IPM motor.

II. Position Estimation Based on Saliency

A. Principle of Estimation

Fig.1 (a) shows an equivalent circuit of an IPM motor. Here, $\boldsymbol{v}$, $\boldsymbol{i}$ and $\boldsymbol{e}_0$ mean the motor voltage and current vectors, and the back electromagnetic force vector on the stator coordinates, respectively.

When the PM motor is driven by a voltage-source PWM inverter, the motor current contains a small amount of harmonic current. The voltage and current vectors can be separated into the fundamental and harmonic components. Because the resistive voltage drop can be neglected, the harmonic equivalent circuit can be approximated by Fig.1

0-7803-4943-1/98/$10.00 © 1998 IEEE

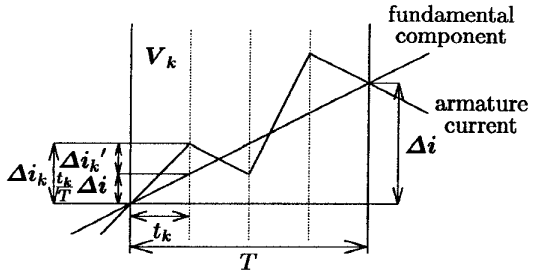

Fig. 2. Armature current waveform.

(b).

$$\tilde{v} = L\frac{d\tilde{i}}{dt}. \tag{1}$$

The above equation indicates that the inductance matrix L can be calculated from the harmonic components of the motor voltage and current vectors, so that the rotor position can be estimated.

The average voltage vector of the PWM inverter is

$$e = \sum \zeta_k V_k \tag{2}$$

where ζ_k means the time ratio of V_k with respect to the modulation period.

$$\zeta_k = \frac{t_k}{T} \tag{3}$$

Therefore, the harmonic voltage vector is equal to a difference between the inverter output voltage vector and the average output voltage vector.

$$V_k' = V_k - e \tag{4}$$

On the other hand, the motor current changes linearly as shown in Fig.2. Since the motor current includes both harmonic and fundamental components, the two components should be separated from each other. The current variation for modulation period is shown by

$$\Delta i = \sum \Delta i_k \tag{5}$$

where $\Delta i_0, \cdots, \Delta i_7$ are the current variations for the intervals of $t_0, \cdots, t_7$, respectively. Assuming that the fundamental component changes linearly in a modulation period, the harmonic component of the current variation can be separated by the following equation.

$$\Delta i_k' = \Delta i_k - \zeta_k \Delta i \tag{6}$$

As a result, we can extract only harmonic components of the voltage and current vectors.

From (1), a relationship between the harmonic components of the voltage vector and the current variation vector is given by

$$L\Delta i_k' = V_k' t_k. \tag{7}$$

Lumping the above equations together over a modulation period gives the following equation.

$$L\left[\begin{array}{cccc} \Delta i_0' & \Delta i_1' & \cdots & \Delta i_7' \end{array}\right] = \left[\begin{array}{cccc} V_0' t_0 & V_1' t_1 & \cdots & V_7' t_7 \end{array}\right] \tag{8}$$

The transposed equation is

$$\left[\begin{array}{c} \Delta i_0'^{\mathrm{T}} \\ \Delta i_1'^{\mathrm{T}} \\ \vdots \\ \Delta i_7'^{\mathrm{T}} \end{array}\right] L^{\mathrm{T}} = \left[\begin{array}{c} V_0'^{\mathrm{T}} t_0 \\ V_1'^{\mathrm{T}} t_1 \\ \vdots \\ V_7'^{\mathrm{T}} t_7 \end{array}\right]. \tag{9}$$

Therefore, the inductance matrix can be calculated as follows:

$$\begin{aligned} L^{\mathrm{T}} &= \left[\begin{array}{c} \Delta i_0'^{\mathrm{T}} \\ \Delta i_1'^{\mathrm{T}} \\ \vdots \\ \Delta i_7'^{\mathrm{T}} \end{array}\right]^{\mathrm{LM}} \left[\begin{array}{c} V_0'^{\mathrm{T}} t_0 \\ V_1'^{\mathrm{T}} t_1 \\ \vdots \\ V_7'^{\mathrm{T}} t_7 \end{array}\right] \\ &= \left[\begin{array}{cc} L_{11} & L_{12} \\ L_{21} & L_{22} \end{array}\right]^{\mathrm{T}} \\ &= \left[\begin{array}{cc} L_0 + L_1 \cos 2\theta & L_1 \sin 2\theta \\ L_1 \sin 2\theta & L_0 - L_1 \cos 2\theta \end{array}\right]. \end{aligned} \tag{10}$$

Here, the "LM" in the above equation is the *left pseudo inverse* operator[9], and it performs the following calculation

$$H^{\mathrm{LM}} = \left(H^{\mathrm{T}} H\right)^{-1} H^{\mathrm{T}}. \tag{11}$$

Therefore, the rotor position can be calculated from the inductance matrix.

$$2\theta = \tan^{-1} \frac{L_{12} + L_{21}}{L_{11} - L_{22}} \tag{12}$$

B. Mathematical meaning of left pseudo inverse

We often use *averaging* when we need a typical value a in a set of quantities $y_1, y_2, \cdots, y_n$.

$$y_1 = a, \quad y_2 = a, \quad \cdots \quad , \quad y_n = a \tag{13}$$

The equations are *over-determined*. The following equation in a matrix form is given by lumping the above equations together.

$$y = \left[\begin{array}{c} y_1 \\ y_2 \\ \vdots \\ y_n \end{array}\right] = \left[\begin{array}{c} 1 \\ 1 \\ \vdots \\ 1 \end{array}\right] a = Ha \tag{14}$$

A solution can be obtained by using the left pseudo inverse.

$$a = H^{\mathrm{LM}} y = (H^{\mathrm{T}} H)^{-1} H^{\mathrm{T}} y = \frac{1}{n} \sum y_k \tag{15}$$

This is the same equation as that of averaging. Therefore, left pseudo inverse includes averaging.

On the other hand, left pseudo inverse also includes *method of least squares*. Let us estimate coefficients of the following equation from a set of data $(x_1, y_1), (x_2, y_2), \cdots, (x_n, y_n)$.

$$y = a + bx \tag{16}$$

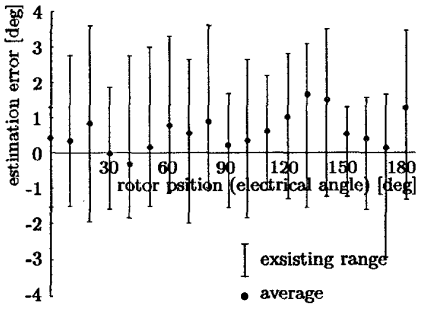

Fig. 3. Experimental result of estimation error.

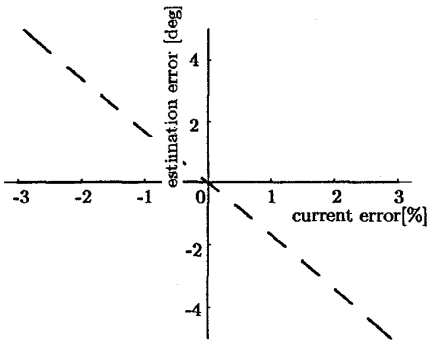

Fig. 4. Estimation error with respect to current detection error.

The matrix-form equation is given by

$$\boldsymbol{y} = \begin{bmatrix} y_1 \\ y_2 \\ \vdots \\ y_n \end{bmatrix} = \begin{bmatrix} 1 & x_1 \\ 1 & x_2 \\ \vdots & \vdots \\ 1 & x_n \end{bmatrix} \begin{bmatrix} a \\ b \end{bmatrix} = \boldsymbol{H} \begin{bmatrix} a \\ b \end{bmatrix}. \quad (17)$$

The left pseudo inverse gives a solution.

$$\begin{aligned} \begin{bmatrix} a \\ b \end{bmatrix} &= \boldsymbol{H}^{\mathrm{LM}}\boldsymbol{y} = (\boldsymbol{H}^{\mathrm{T}}\boldsymbol{H})^{-1}\boldsymbol{H}^{\mathrm{T}}\boldsymbol{y} \\ &= \begin{bmatrix} \sum 1 & \sum x_k \\ \sum x_k & \sum x_k^2 \end{bmatrix}^{-1} \begin{bmatrix} 1 & 1 & \cdots & 1 \\ x_1 & x_2 & \cdots & x_n \end{bmatrix} \begin{bmatrix} y_1 \\ y_2 \\ \vdots \\ y_n \end{bmatrix} \\ &= \begin{bmatrix} \sum 1 & \sum x_k \\ \sum x_k & \sum x_k^2 \end{bmatrix}^{-1} \begin{bmatrix} \sum y_k \\ \sum x_k y_k \end{bmatrix} \end{aligned} \quad (18)$$

This coincides with the solution obtained from the method of least squares.

The above consideration indicates that the inductance matrix obtained from (10) is an optimum solution in view of the minimum error square.

III. Analysis of Estimation Error

Fig.3 shows experimental results of estimation errors at a standstill. A bullet and the corresponding vertical bar mean the average value and an existing range of estimated position, respectively, obtained from 15 trials at a rotor position. These experimental results have demonstrated that the proposed approach has the capacity of estimating the rotor position with an error of less than 4° in electrical angle at a standstill. The average value of the estimation error is within 2°, and the deviation from the average value is less than 3°.

In the proposed position estimation at a standstill, the inductance matrix and the rotor position are calculated from six current variation vectors $\Delta\boldsymbol{i}_1, \cdots, \Delta\boldsymbol{i}_6$, each digital signal of which is obtained by current sensors and A/D converters. Therefore, errors in the digital signals of the current variations cause an estimation error. This section analyzes the estimation error.

A. Resolution of A/D converters

All digital signals of the current variations contain a quantization error of A/D converters. Fig.4 shows an analytical result of the estimation error at $\theta = 0$, when a current error occurs in the β-component of $\Delta\boldsymbol{i}_6'$ among the six current variation vectors. The current error is expressed as a percentage to the rated current of the tested motor. It is assumed that the average output voltage vector $\boldsymbol{e}$ is equal to zero vector. The list of Mathematica Notebook file for the analysis is shown in Fig.5.

The analytical result illustrates that an estimation error of 5° in electrical angle is generated by a current error of 3% in only one digital signal among the 12 digital signals. The same analysis is performed, concerning the other 11 digital signals. It is confirmed that the estimation error in the case of Fig.4 is the largest among them. Since the quantization errors occur at random, all the estimation errors generated by each digital signal have the same polarity in the worst case. Therefore, it is considered that the sufficient condition for getting an accuracy of position estimation within 5° is that resolution of the A/D converters for current detection is less than 3%/12=0.25% of the rated current. In the experimental system, since the resolution of the A/D converters corresponds to 0.2% of the rated current, the analytical result almost coincides with the experimental result.

B. Magnetic saliency ratio

Although it can be understood easily that the position estimation based on magnetic saliency is not applicable to a cylindrical machine, no paper has discussed how much the magnetic saliency ratio is necessary to achieve the position estimation as far as the authors know. Here, we investigate a relationship between the magnetic saliency ratio and estimation error under the condition that a current error of -3% is included in $\Delta i_{6\beta}'$, which corresponds to Fig.4. Generally, q-axis inductance of an IPM motor is greater than d-axis inductance. Therefore, the magnetic saliency ratio is defined as L_q/L_d.

Fig.6 shows an analytical result of a position estima-

```
■ Initialize
Ed=280 ; Tpwm=3000 ;
L0=0.1655 ; L1=-0.0405 ;
id=0.7;
t1=t2=t3=t4=t5=t6=1/6/Tpwm ;
x=0 ; y=2 Pi x / 180 ;
ga=. ; gb=. ;
■ Calculation of harmonic currents
■ switching states
s1={1,0,0} ;s2={0,1,0} ;s3={1,1,0} ;
s4={0,0,1} ;s5={1,0,1} ;s6={0,1,1} ;
■ voltage vectors
Cab=Sqrt[2/3]{{1,-1/2,-1/2},{0,Sqrt[3]/2,-Sqrt[3]/2}} ;
v1=Ed Cab.s1 ; v2=Ed Cab.s2 ; v3=Ed Cab.s3 ;
v4=Ed Cab.s4 ; v5=Ed Cab.s5 ; v6=Ed Cab.s6 ;
■ product of voltage vectors and times
v={v1,v2,v3,v4,v5,v6} ;
t={t1,t2,t3,t4,t5,t6} ;
vt=v t ;
■ inverse of inductance matrix
LL={{L0-L1 Cos[y],-L1 Sin[y]},
{-L1 Sin[y],L0+L1 Cos[y]}}/(L0^2-L1^2) ;
■ current variations including some errors
i1=N[LL.v1 t1] ; i2=N[LL.v2 t2] ; i3=N[LL.v3 t3] ;
i4=N[LL.v4 t4] ; i5=N[LL.v5 t5] ;
i6=N[LL.v6 t6 + {id*ga,id*gb}] ;
■ Estimation of inductance matrix and rotor position
H={i1,i2,i3,i4,i5,i6} ;
HLM=Inverse[Transpose[H].H].Transpose[H] ;
HLM.vt ;
{{L11,L12},{L21,L22}}=% //N ;
z=ArcTan[(L12+L21)/(L11-L22)]*180/(2*Pi) //N ;
ga=0 ; gb=. ;
z=Plot[z,{gb,-0.03,0.03},Prolog -> Dashing[{0.05,0.05}],
PlotRange -> {{-0.03,0.03},{-5,5}}];
```

Fig. 5. List of Mathematica Notebook file for analysis of estimation error.

tion error against the magnetic saliency ratio. A bullet in the figure indicates the tested motor with a magnetic saliency ratio of 1.65. As the magnetic saliency ratio decreases, the estimation error increases and the estimation error amounts to 2 times at 1.25. If the ratio decreases from this point, the estimation error increases more and more, and it becomes impossible to estimate the rotor position in practice. On the other hand, even though the magnetic saliency ratio increases, the estimation error hardly decreases. For example, in order to get 2 times of estimation accuracy compared with that of the tested motor, we need a motor with a magnetic saliency ratio of 6.5. It is considered that the magnetic saliency ratio larger than 1.5 is enough to estimate the rotor position.

C. Gain error in current detection circuit

At the time of detecting a digital signal of current variation, an error may be caused in a current sensor and a detection circuit along with a quantization error of the A/D converters. Fig.7 shows an analytical result and an experimental result in the case that gain of the α-axis current detection circuit is 95% of that of the β-axis. This result illustrates that a gain error of 5% generates a sinusoidal position estimation error having an amplitude of 3°. Moreover, coincidence between the analytical and experimental results shows propriety of this analysis. In a practical system, it is necessary to be careful of accuracy of the current sensors and the current detection circuits.

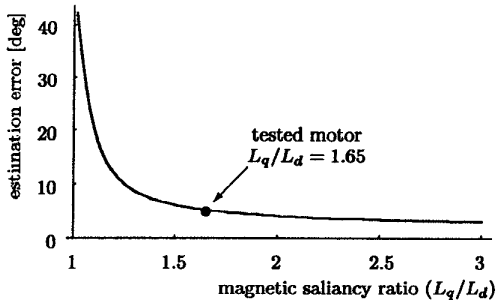

Fig. 6. Effect of magnetic saliency on estimation error (current detected error: −3%).

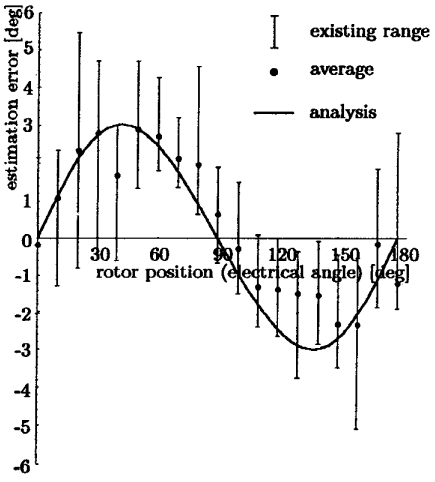

Fig. 7. Exprimental result of estimation error when the current detection circuit has a gain error.

IV. PWM SCHEME USING REDUNDANT VOLTAGE VECTORS

In order to perform precise position estimation, the authors have proposed a novel PWM scheme using redundant voltage vectors [7]. The average voltage vector during a modulation period can be expressed by

$$e = \sum s_k \zeta_k V_k \tag{19}$$

$$\sum s_k \zeta_k = 1 \tag{20}$$

Here, s_k, which takes a value of 1 or 0 during the modulation period, indicates whether V_k is selected as an output vector or not, respectively. Lumping the equations together gives the following equation.

$$\begin{bmatrix} e_\alpha \\ e_\beta \\ 1 \end{bmatrix} = \begin{bmatrix} s_0 V_{0\alpha} & s_1 V_{1\alpha} & \cdots & s_7 V_{7\alpha} \\ s_0 V_{0\beta} & s_1 V_{1\beta} & \cdots & s_7 V_{7\beta} \\ s_0 & s_1 & \cdots & s_7 \end{bmatrix} \begin{bmatrix} \zeta_0 \\ \zeta_1 \\ \vdots \\ \zeta_7 \end{bmatrix} \tag{21}$$

In the above equation, ζ_k has to be decided so that the PWM inverter produces the average voltage vector e during

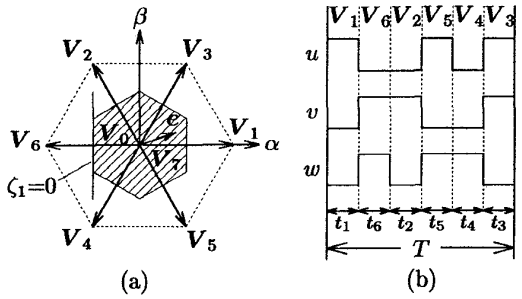

Fig. 8. PWM suitable for position estimation in a low-speed range. (a) voltage vectors. (b) PWM pattern.

the modulation period. No general solution to (21) exists because the number of unknown variables is more than the number of equations. However, introduction of a *right pseudo inverse* matrix[9] enables to solve ζ_k as follows:

$$\begin{bmatrix} \zeta_0 \\ \zeta_1 \\ \vdots \\ \zeta_7 \end{bmatrix} = \begin{bmatrix} s_0V_{0\alpha} & s_1V_{1\alpha} & \cdots & s_7V_{7\alpha} \\ s_0V_{0\beta} & s_1V_{1\beta} & \cdots & s_7V_{7\beta} \\ s_0 & s_1 & \cdots & s_7 \end{bmatrix}^{\mathrm{RM}} \begin{bmatrix} e_\alpha \\ e_\beta \\ 1 \end{bmatrix} \tag{22}$$

where

$$\boldsymbol{F}^{\mathrm{RM}} = \boldsymbol{F}^{\mathrm{T}} \left(\boldsymbol{F}\boldsymbol{F}^{\mathrm{T}} \right)^{-1} \tag{23}$$

As a result of the calculation, one can decide a suitable PWM pattern under any combination of $\boldsymbol{V}_k$ during the modulation period. Assigning each actual value to $\boldsymbol{V}_k$ gives the matrix $\boldsymbol{F}$ as follows:

$$\begin{aligned} \boldsymbol{F} &= \begin{bmatrix} s_0V_{0\alpha} & s_1V_{1\alpha} & \cdots & s_7V_{7\alpha} \\ s_0V_{0\beta} & s_1V_{1\beta} & \cdots & s_7V_{7\beta} \\ s_0 & s_1 & \cdots & s_7 \end{bmatrix} \\ &= \begin{bmatrix} 0 & \frac{2E_d}{\sqrt{6}}s_1 & -\frac{E_d}{\sqrt{6}}s_2 & \frac{E_d}{\sqrt{6}}s_3 & & \\ 0 & 0 & \frac{E_d}{\sqrt{2}}s_2 & \frac{E_d}{\sqrt{2}}s_3 & * & \\ s_0 & s_1 & s_2 & s_3 & & \\ & -\frac{E_d}{\sqrt{6}}s_4 & \frac{E_d}{\sqrt{6}}s_5 & \frac{2E_d}{\sqrt{6}}s_6 & 0 & \\ * & -\frac{E_d}{\sqrt{2}}s_4 & -\frac{E_d}{\sqrt{2}}s_5 & 0 & 0 & \\ & s_4 & s_5 & s_6 & s_7 & \end{bmatrix} \end{aligned} \tag{24}$$

Here, E_d means the dc link voltage of the inverter.

A. PWM pattern in lower-speed range

In order to calculate the inductance matrix $\boldsymbol{L}$ with enough accuracy, the harmonic voltage and current are desirable to contain various directional components. Fig.8 (b) shows a PWM pattern suitable for position estimation in a lower-speed range. Only this PWM pattern was used in the experimental system shown in reference [8]. Note that the PWM pattern consists of six non-zero voltage vectors and that the inverter selects neither $\boldsymbol{V}_0$ nor $\boldsymbol{V}_7$.

$$s_1 = s_2 = \cdots = s_6 = 1, \quad s_0 = s_7 = 0 \tag{25}$$

Therefore, the right pseudo inverse can be calculated from (23) and (24).

$$\begin{aligned} &\left(\boldsymbol{F}\boldsymbol{F}^{\mathrm{T}}\right)^{-1} \\ &= \begin{bmatrix} \sum s_k^2V_{k\alpha}^2 & \sum s_k^2V_{k\alpha}V_{k\beta} & \sum s_k^2V_{k\alpha} \\ \sum s_k^2V_{k\alpha}V_{k\beta} & \sum s_k^2V_{k\beta}^2 & \sum s_k^2V_{k\beta} \\ \sum s_k^2V_{k\alpha} & \sum s_k^2V_{k\beta} & \sum s_k^2 \end{bmatrix}^{-1} \\ &= \begin{bmatrix} 2E_d^2 & 0 & 0 \\ 0 & 2E_d^2 & 0 \\ 0 & 0 & 6 \end{bmatrix}^{-1} = \frac{1}{6E_d^2} \begin{bmatrix} 3 & 0 & 0 \\ 0 & 3 & 0 \\ 0 & 0 & E_d^2 \end{bmatrix} \end{aligned} \tag{26}$$

$$\boldsymbol{F}^{\mathrm{RM}} = \boldsymbol{F}^{\mathrm{T}} \left(\boldsymbol{F}\boldsymbol{F}^{\mathrm{T}}\right)^{-1} = \left[\begin{array}{c} \frac{1}{2\sqrt{6}E_d} \begin{bmatrix} 0 & 2 & -1 & 1 & -1 & 1 & -2 & 0 \\ 0 & 0 & \sqrt{3} & \sqrt{3} & -\sqrt{3} & -\sqrt{3} & 0 & 0 \end{bmatrix} \\ \frac{1}{6}\begin{bmatrix} 0 & 1 & 1 & 1 & 1 & 1 & 1 & 0 \end{bmatrix} \end{array} \right]^{\mathrm{T}} \tag{27}$$

The right pseudo inverse gives $\zeta_0, \zeta_1, \cdots, \zeta_7$. For example, the following equation decides ζ_1 from (27).

$$\zeta_1 = \frac{1}{\sqrt{6}E_d}e_\alpha + \frac{1}{6} \tag{28}$$

However, all of ζ_k should satisfy $0 < \zeta_k < 1$ to generate the PWM signal properly. Since $\zeta_1 < 0$ when e_α is smaller than $-E_d/\sqrt{6}$, which corresponds to half of $\boldsymbol{V}_6$, the inverter can not produce an average voltage vector located on the left-half plain divided by a line indicated as $\zeta_1 = 0$ in Fig.8 (a). In the same way, the average output voltage vector is investigated concerning the other ζ_k.

In Fig.8 (a), hatching indicates an area of the average voltage vector that can be produced by using the PWM pattern of Fig.8 (b). It is shown that this PWM pattern can not be used in a higher-speed range in which an amplitude of the inverter output voltage is larger than half of the rated output voltage. Although the PWM pattern gives excellent position estimation characteristics in a lower-speed range, using only one PWM pattern consisting of six non-zero voltage vectors restricts to driving the IPM motor and estimating the rotor position in a higher-speed range.

B. PWM pattern in higher-speed range

Fig.9 (b) shows the PWM pattern used in a higher-speed range. The PWM pattern consists of 4 voltage vectors including a zero vector.

$$s_0 = s_1 = s_3 = s_5 = 1, \quad s_2 = s_4 = s_6 = s_7 = 0 \tag{29}$$

Therefore, we can obtain the right pseudo inverse as follows.

$$\begin{aligned} \left(\boldsymbol{F}\boldsymbol{F}^{\mathrm{T}}\right)^{-1} &= \begin{bmatrix} E_d^2 & 0 & \frac{4}{\sqrt{6}}E_d \\ 0 & E_d^2 & 0 \\ \frac{4}{\sqrt{6}}E_d & 0 & 4 \end{bmatrix}^{-1} \\ &= \frac{1}{E_d^2} \begin{bmatrix} 3 & 0 & -\frac{3}{\sqrt{6}}E_d \\ 0 & 1 & 0 \\ -\frac{3}{\sqrt{6}}E_d & 0 & \frac{3}{4}E_d^2 \end{bmatrix} \end{aligned} \tag{30}$$

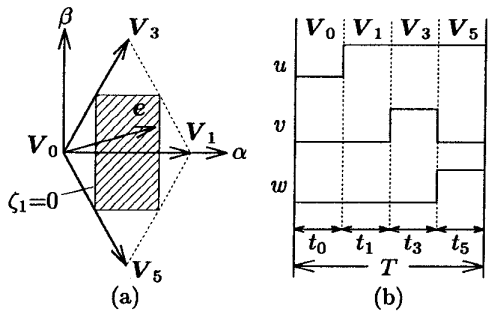

Fig. 9. PWM suitable for position estimation in a high-speed range. (a) voltage vectors. (b) PWM pattern.

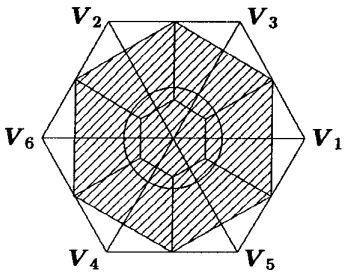

Fig. 10. Selection of PWM patterns.

$$\boldsymbol{F}^{\mathrm{RM}} = \boldsymbol{F}^{\mathrm{T}}\left(\boldsymbol{F}\boldsymbol{F}^{\mathrm{T}}\right)^{-1} = \left[\begin{array}{c} \frac{1}{\sqrt{6}E_d}\begin{bmatrix} -3 & 3 & 0 & 0 & 0 & 0 & 0 & 0 \\ 0 & 0 & 0 & \sqrt{3} & 0 & -\sqrt{3} & 0 & 0 \end{bmatrix} \\ \frac{1}{4}\begin{bmatrix} 3 & -1 & 0 & 1 & 0 & 1 & 0 & 0 \end{bmatrix} \end{array}\right]^{\mathrm{T}} \tag{31}$$

The right pseudo inverse gives ζ_k. For example, the following equation decides ζ_1.

$$\zeta_1 = \frac{3}{\sqrt{6}E_d}e_\alpha - \frac{1}{4} \tag{32}$$

Since $0 < \zeta_1$, e_α has to be larger than $E_d/(2\sqrt{6})$, which corresponds to a quarter of $\boldsymbol{V}_1$. In Fig.9 (a), hatching indicates an available area of the PWM pattern shown in Fig.9 (b).

The PWM pattern of Fig.9 (b) is used when the phase of $\boldsymbol{e}$ exists between 30° and −30°. Six kinds of PWM patterns symmetrical to Fig.9 (b) are switched over every 60° in the phase of the average output voltage vector $\boldsymbol{e}$ as shown in Fig.10. In this experiment, the PWM pattern of Fig.8 (a) is used in a speed range less than half of the rated speed, which corresponds to inside of a circle in Fig.10. On the other hand, the switchover of the six symmetrical PWM patterns is used in a speed range more than half of the rated speed. In Fig.10, hatching indicats a total available area of the average voltage vector, which is the same as that of a conventional sinusoidal PWM[10].

Precise position estimation in a wide-speed range from zero to the rated speed can be realized by selecting one of seven PWM patterns, which depends on the amplitude and phase angle of the average output voltage vector $\boldsymbol{e}$.

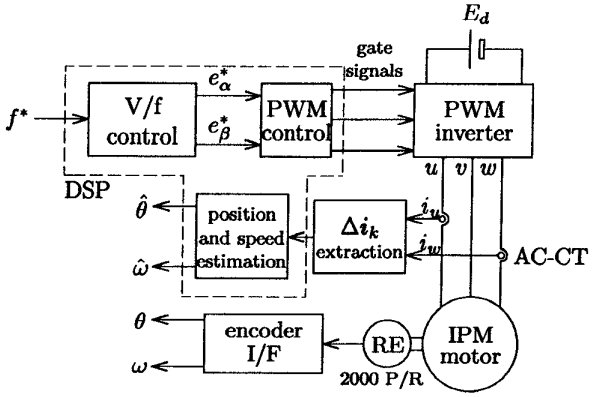

Fig. 11. System configuration.

TABLE I
SYSTEM PARAMETERS OF THE EXPERIMENTAL SYSTEM.

number of pole		4	
armature resistance	r	15	Ω
d-axis inductance	L_d	125	mH
q-axis inductance	L_q	206	mH
rated power		100	W
rated speed		1500	rpm
modulation period	T	333	μs
dc link voltage	E_d	280	V

V. System Configuration

Fig.11 and Table I show an experimental system and the system parameters, respectively. The control circuit is composed of a digital circuit, including a DSP (ADSP-2101, Analog Devices), except for a $\Delta\boldsymbol{i}_k$ extraction stage.

The current deviation vectors $\Delta\boldsymbol{i}_k$ are extracted from the motor current signals detected by two current sensors AC-CTs, and the digital controller estimates the rotor position $\hat{\theta}$ from PWM signals and $\Delta\boldsymbol{i}_k$. Furthermore, the estimated speed $\hat{\omega}$ is calculated from a difference of the estimated position during an estimation period. This system constitutes an open-loop control system in which the ratio of motor voltage and frequency is maintained constant. Corresponding to the frequency command f^*, the inverter voltage references, e^*_α and e^*_β, are generated, and the gate signals shown in Fig.8 and Fig.9 are synthesized by the proposed PWM control. On the other hand, the rotary encoder (RE), which is attached to the IPM motor, gives an actual position θ and an actual speed ω for measurement.

VI. Experimental Results

Fig.12 shows waveforms of the actual position and the estimated position in electrical angle where the IPM motor is driven at a low speed of 90 rpm. In this case, the PWM pattern of Fig.8 is used. Fig.13 shows waveforms of the actual position and the estimated position at the rated speed of 1500 rpm. Here, the voltage-source inverter generates

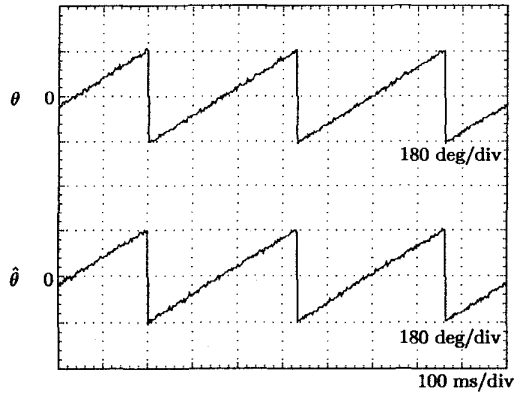

Fig. 12. Position estimation characteristics (90 rpm). Upper trace: actual position θ, Lower trace: estimated position $\hat{\theta}$.

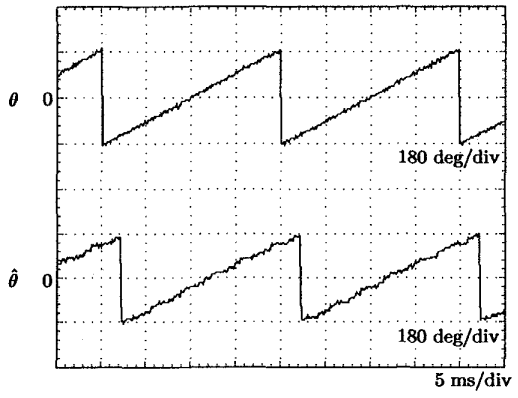

Fig. 13. Position estimation characteristics (1500 rpm). Upper trace: actual position θ, Lower trace: estimated position $\hat{\theta}$.

the PWM pattern shown in Fig.9. The experimental results show that satisfactory position estimation is achieved in both the low-speed and the rated-speed operations. It is confirmed experimentally that selecting one of the seven PWM patterns by the amplitude and phase of e enables to estimate the position in a wide-speed range from zero to the rated speed. The estimated position contains some phase delay with respect to the actual position. The delay is caused by the estimation period (666 μs) and low pass filters (200 Hz) to remove electrical noise components from the signals.

Fig.14 shows a position estimation performance when the PWM pattern for lower-speed rage is switched over to that for higher-speed range. It is shown that a good position estimation performance is obtained without any transient phenomena even when the PWM pattern is switched over.

VII. Conclusion

This paper has discussed a position-sensorless IPM motor drive system introducing real-time position estimation based on magnetic saliency, which has already been proposed by the authors [7][8]. Selecting one of seven PWM patterns expands the speed range capable of estimating the rotor position to higher-speed range. The PWM pattern is switched over, depending on an amplitude and phase of the average output voltage vector. The selection was implemented into a digital controller for an IPM motor (100 W), and the position estimation performance was tested. As a result, experimental results demonstrate that the selection of the PWM pattern makes it possible to estimate the rotor position in a wide-speed range from zero to the rated speed.

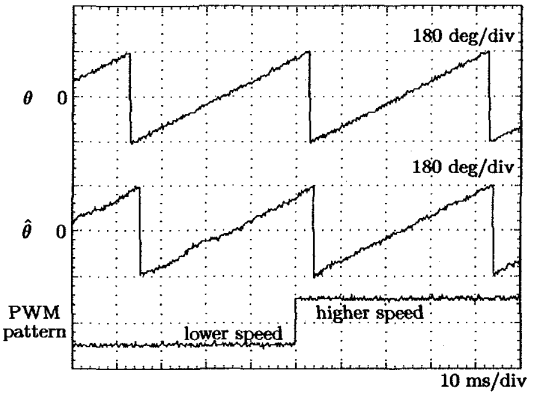

Fig. 14. Position estimation characteristics when PWM pattern is switched over. Upper trace: actual position θ, Middle trace: estimated position $\hat{\theta}$, Lower trace: digital signal indicating PWM pattern.

References

[1] N. Matsui, and T. Takeshita: "A Novel Starting Method of Sensorless Salient-Pole Brushless Motor," *IEEE/IAS Annual Meeting*, pp. 386–392, 1994.

[2] P. L. Jansen, and R. D. Lorenz: "Transducerless Position and Velocity Estimation in Induction and Salient AC Machines," *IEEE Trans. Ind. Appl.*, Vol. 31, No. 2, pp. 240–247, 1995.

[3] M. J. Corley, and R. D. Lorenz: "Rotor Position and Velocity Estimation for a Permanent Magnet Synchronous Machine at standstill and high Speeds," *IEEE/IAS Annual Meeting*, pp. 36-41, 1996.

[4] S. Kondo, A. Takahashi, and T. Nishida: "Armature Current Locus Based Estimation Method of Rotor Position of Permanent Magnet Synchronous Motor without Mechanical Sensor," *IEEE/IAS Annual Meeting*, pp. 55–60, 1995.

[5] F.Blashke, J. van der Burgt, A. Vandenput: "Sensorless Direct Field Orientation at Zero Flux Frequency," *IEEE/IAS Annual Meeting*, pp. 189–196, 1996.

[6] Manfred Schroedl: "Sensorless Control of AC Machines at Low Speed and Standstill Based on the "INFORM" Method," *IEEE/IAS Annual Meeting*, pp. 270–277, 1996.

[7] S. Ogasawara, and H. Akagi: "An Approach to Real-Time Position Estimation at Zero and Low Speed for a PM Motor Based on Saliency," *IEEE Trans. Ind. Applicat.*, vol. 34, pp. 163–168, Jan./Feb. 1998.

[8] S. Ogasawara, and H. Akagi: "Implementation and Position Control Performance of a Position-Sensorless IPM Motor Drive System Based on Magnetic Saliency," *IEEE Trans. Ind. Applicat.*, vol. 34, No. 4, Jul./Aug. 1998.

[9] S.Wolfram: "Mathematica: A System for Doing Mathematics by Computer —Second Edition—," Addison-Wesley, 1991.

[10] S. Ogasawara, H. Akagi and A. Nabae: "A Novel PWM Scheme of Voltage Souce Inverters Based on Space Vector Theory," *Proc. of EPE'89*, pp. 1197–1202, 1989.